Original Article doi: 10.2176/nmc.oa.2018-0054

Neurol Med Chir (Tokyo) 58, 384–392, 2018 Online August 3, 2018

Metabolomic Analysis of Mouse Brain after a Transient Middle Cerebral Artery Occlusion by Mass Spectrometry Imaging

Takatsugu ABE,[1] Kuniyasu NIIZUMA,[1,2,3] Atsushi KANOKE,[1] Daisuke SAIGUSA,[4] Ritsumi SAITO,[4] Akira URUNO,[4] Miki FUJIMURA,[1] Masayuki YAMAMOTO,[4] and Teiji TOMINAGA[1]

[1]*Department of Neurosurgery, Tohoku University Graduate School of Medicine, Sendai, Miyagi, Japan;*
[2]*Neurosurgical Engineering and Translational Neuroscience, Tohoku University Graduate School of Medicine, Sendai, Miyagi, Japan;*
[3]*Department of Neurosurgical Engineering and Translational Neuroscience, Graduate School of Biomedical Engineering, Tohoku University, Sendai, Miyagi, Japan;*
[4]*Department of Medical Biochemistry, Tohoku University Graduate School of Medicine, Sendai, Miyagi, Japan*

Abstract

We performed metabolomic analyses of mouse brain using a transient middle cerebral artery occlusion (tMCAO) model with Matrix Assisted Laser Desorption/Ionization (MALDI)-mass spectrometry imaging (MSI) to reveal metabolite changes after cerebral ischemia. We selected and analyzed three metabolites, namely creatine (Cr), phosphocreatine (P-Cr), and ceramides (Cer), because these metabolites contribute to cell life and death. Eight-week-old male C57BL/6J mice were subjected to tMCAO via the intraluminal blockade of the middle cerebral artery (MCA) and reperfusion 60 min after the induction of ischemia. Each mouse was randomly assigned to one of the three groups; the groups were defined by the survival period after reperfusion: control, 1 h, and 24 h. Corrected samples were analyzed using MALDI-MSI. Results of MSI analysis showed the presence of several ionized substances and revealed spatial changes in some metabolites identified as precise substances, including Cr, P-Cr, Cer d18:1/18:0, phosphatidylcholine, L-glutamine, and L-histidine. Cr, P-Cr, and Cer d18:1/18:0 were changed after tMCAO, and P-Cr and Cer d18:1/18:0 accumulated over time in ischemic cores and surrounding areas following ischemia onset. The upregulation of P-Cr and Cer d18:1/18:0 was detected 1 h after tMCAO when no changes were evident on hematoxylin and eosin staining and immunofluorescence assay. P-Cr and Cer d18:1/18:0 can serve as neuroprotective therapies because they are biomarker candidates for cerebral ischemia.

Key words: ceramide, cerebral ischemia, mass spectrometry imaging, metabolomic analysis, phosphocreatine

Introduction

Cerebral infarction (CI) causes high morbidity and mortality, and the number of patients with CI has been increasing. Recent advances in thrombolytic therapies and mechanical thrombectomy have significantly improved patient outcomes, but these innovations are applicable to < 10% of patients because of their associated short therapeutic time windows. Most patients without such revascularization therapy develop CI; thus, an understanding of changes to the various signaling pathways after the acute CI remains important for developing neuroprotection therapies and improving patient outcomes.

Classically, various signaling pathways after stroke are analyzed mainly at the message level using polymerase chain reaction or at the protein level using immunohistochemistry and Western blotting. These classical methods require specific probes or antibodies. Advancements in mass spectrometric analysis allow us to determine the expression of small metabolites and phospholipids after CI without probes.[1,2] Mass spectrometry (MS) techniques, such

Received March 2, 2018; Accepted July 2, 2018

as liquid chromatography-MS (LC-MS), and gas chromatography-MS (GC-MS) have been used as metabolomic methods.[3,4] However, these techniques cannot directly evaluate the spatial distributions of metabolites. Recently, matrix-assisted laser desorption/ionization (MALDI)-mass spectrometry imaging (MSI) has been used to display the spatial distributions of various biomolecules without labeling during a single analysis,[5–9] and the expression of some metabolites after brain injuries has been reported.[2,10]

The central objective of this study was to analyze metabolomic changes after transient middle cerebral artery occlusion (tMCAO) in mice using MALDI-MSI. We focused on creatine (Cr), phosphocreatine (P-Cr), and ceramides (Cer) because these substances may be involved in cell life and death.

Materials and Methods

Experimental animal model

All animals were treated in accordance with the Code of Ethics of the World Medical Association as well as the Tohoku University Guidelines on the basis of the International Guiding Principles for Biomedical Research Involving Animals. The animal protocols were approved by the Tohoku University's Administrative Panel on Laboratory Animal Care.

Eight-week-old male C57BL/6J mice (20.2–24.0 g) were subjected to tMCAO by the intraluminal blockade of the middle cerebral artery (MCA) as previously described.[11] Animals were anesthetized with 1.5% isoflurane in 30% oxygen and 70% nitrous oxide during spontaneous breathing. Rectal temperatures during all surgical procedures were maintained at 37 ± 0.5°C using a feedback-regulated heating pad (BWT-100, Bio Research Center, Nagoya). A midline skin incision was made, and the left common carotid artery (CCA), internal carotid artery (ICA), pterygopalatine artery (PPA), and external carotid artery (ECA) were carefully dissected in the supine position. The ICA and CCA were temporarily closed using a vascular clip (MH-1-20, BEAR Medic, Tokyo), and a silicon-coated 6-0 nylon monofilament (602345PK5Re, Doccol, Redlands, CA, USA) was introduced into the arteriotomy hole in the ECA and advanced to the CCA bifurcation. After the vascular clip was removed and the ECA was cut, the intraluminal suture was inserted into the ICA until mild resistance was felt. The collar suture of the ECA stump was securely tightened around the inserted suture. The PPA was coagulated and cut to reduce variations within the ischemic area.[12] The wound was closed using 6-0 nylon sutures. The mouse was placed in a prone position, and the scalp was cut to expose the thin skull over the bilateral cerebral and cerebellar hemispheres. The surface of the skull was covered with a slipcover over a thin layer of saline to prevent drying. We measured the cerebral blood flow (CBF) values through the intact skull using laser speckle flowmetry (OMEGAZONE, Omegawave, Tokyo) and confirmed decreasing CBF values in the MCA and posterior cerebral artery territories (Fig. 1A). The mouse was then allowed to regain consciousness, after that it was re-anesthetized and placed in a supine position and the intraluminal suture was gently and slowly withdrawn to achieve reperfusion 60 min after the induction of ischemia. The ECA was ligated with a collar suture. Each mouse was randomly assigned to one of three groups, which were defined by survival period after reperfusion: control (n = 3), 1 h (n = 3), and 24 h (n = 3). The treated mice were awakened and allowed a predetermined survival period according to the assigned group. Intact mice were used as a control group.

MSI materials

Carboxymethylcellulose (CMC) sodium salt was purchased from Wako Pure Chemical Industries (Osaka). Molecular sieves, 13X, beads were purchased from NACALAI TESQUE (Kyoto). α-Cyano-4-hydroxycinnamic acid (CHCA) was purchased from Sigma-Aldrich (Tokyo). The chemical standard of sodium creatine phosphate hydrate and ceramides were purchased from TCI (Tokyo) and Avanti Polar Lipids (Alabaster, AL, USA).

Tissue preparation

Cold saline was perfused into the heart of anesthetized mice at 1 or 24 h after reperfusion according to the assigned group. Control mice were sacrificed without reperfusion. To prevent the progression of postmortem metabolism, the brain was rapidly removed, placed in a 5 mL microtube, and froze the tissue in liquid nitrogen. The frozen tissues were stored at −80°C until sectioning. The samples were set on a cryostat with 4% CMC. Tissue sections for MSI analyses were cut by cryostat at 1.00, 1.80, and 2.50 mm posterior to the bregma (8-μm thickness, two continuous sections each for the scan range; m/z 85–305 and 520–820, respectively). To compare spatially metabolomic states between the ipsilateral and contralateral hemispheres of the MCAO brain, the frozen brains were dissected into coronal sections. To compare temporal metabolomic changes, each section harvested from mice within the control, 1 h, and 24 h groups were placed on a glass slide and simultaneously analyzed. The glass slide was coated with indium–tin oxide (100 Ω^{-2}; Matsunami, Osaka) and stored at −80°C in a 50 mL tube with molecular sieves, 13X, beads until MSI analysis. The region

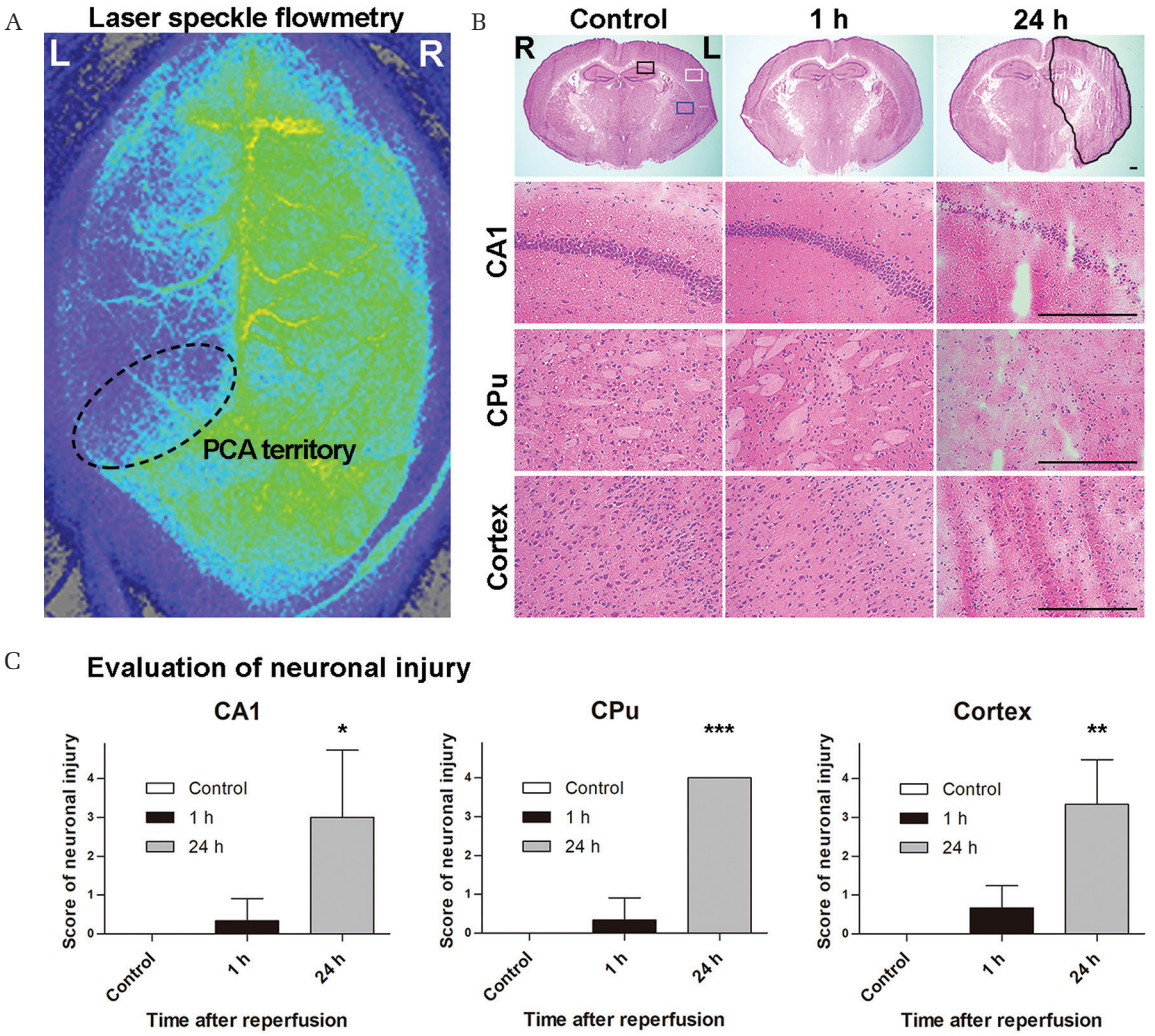

Fig. 1 Assessment of the ischemic area after transient middle cerebral artery occlusion (tMCAO). (A) Laser speckle flowmetry shows signal attenuation in the perfusion area of the middle and posterior cerebral arteries, indicating decreased cerebral blood flow in the tMCAO model. (B) Hematoxylin and eosin staining over time after tMCAO. Hippocampal CA1 (CA1), caudoputamen (CPu), and cerebral cortex (Cortex) are presented as *black*, *blue*, and *white square* regions, respectively. The black free line region indicates an area of infarction with neuronal cell loss and tissue damage. One hour after tMCAO, no obvious changes are observed compared with controls. However, neural cells of the CA1, CPu, and cerebral cortex are decreased 24 h after tMCAO. These sections are 1.80-mm posterior to the bregma. The scale bars are 300 µm. (C) These graphs show the score of neuronal injury in the hippocampal CA1, CPu, and the cerebral cortex on the scales of 0–4. All lesions exhibited significant neuronal cell damage 24 h after tMCAO. *$P < 0.05$, **$P < 0.01$, and ***$P < 0.001$ ($N = 3$ each).

of laser irradiation for MSI analysis was set under the observation by light microscope before sample preparation for MALDI-MSI analysis. Each sample was then deposited with a matrix (0.7-µm thickness from 660 mg of CHCA) using iMLayer (Shimadzu, Kyoto). For histological stain and MSI analyses, frozen brains were prepared as 8-µm cryosections on glass slides at −25°C using cryostat (CM3050S, Leica, Heidelberger, Germany), and the sample sections were then processed for hematoxylin and eosin (HE) and immunofluorescence staining. HE staining was routinely performed, and the slides were microscopically captured (DFC7000 T, Leica, Tokyo). To grade the neuronal damage qualitatively, we assessed neuronal cells in hippocampus, caudoputamen (CPu), and the cerebral cortex on the scales of 0–4. For the hippocampal lesion, we graded the neuronal damage on a scale with 0 = no damage; 1 = scattered ischemic neurons in CA1 subregion; 2 = moderate ischemic damage in CA1 subregion; 3 = whole pyramidal cells damaged in CA1 subregion; and 4 = extensive cell damage in all hippocampal

subregions.[13] For the CPu and the cerebral cortex, we graded the neuronal damage on a scale with 0 = normal; 1 = 0–25% neurons damaged; 2 = 25–50% neurons damaged; 3 = 50–75% neurons damaged; and 4 = 75–100% neurons damaged.[14]

Immunofluorescence

Injured cells were visualized using terminal deoxynucleotidyl transferase dUTP nick-end labeling (TUNEL) staining (In situ cell death detection kit, fluorescein, 11684795910, Roche, Tokyo). Neuronal cells were stained with an anti-NeuN antibody (MAB377, Millipore, MA, USA). All sections were fixed with 4% paraformaldehyde in phosphate-buffered saline (PBS) for 20 min at room temperature (RT) and blocked with 20% BLOCK ACE (UKB40, DS Pharma, Osaka), 5% bovine serum albumin, and 0.3% TritonX-100 (X100-500 ML, Sigma-Aldrich, MO, USA) for 30 min at RT. They were washed using PBS with 0.1% Tween-20 each time. The sections were incubated with an anti-NeuN antibody (1:50) overnight at 4α and secondarily with a donkey anti-mouse IgG, Alexa Fluor 594 (1:200, A21203, Invitrogen, CA, USA) for 1 h at RT. They were incubated with the TUNEL kit for 1 h at 37°C and enclosed with ProLong Diamond Antifade Mountant with DAPI (P36962, Thermo Fisher Scientific, MA, USA). Photographs of sections were captured using a confocal microscope (C2, Nikon, Tokyo).

MALDI-MSI analysis of phospholipids

Mass spectra were acquired with a MALDI-MSI system; iMScope (Shimadzu) using two glass slides, each of which included three slices of the brain for two scan ranges, namely *m/z* 85–305 and *m/z* 520–820. MSI conditions are shown in Table 1. The laser irradiation times, laser power, laser irradiation diameter, laser frequency, detection voltage, sample voltage, and the accumulated number of MALDI-MSI were 100 shots, 45, 25 µm, 1000 Hz, 2.1, 3.5 kV, and 1/pixel, respectively. A raster scan on the tissue surface was automatically performed (141 × 171 average pixels per scan). The average spatial interval of data points out of a total of 24,039 data points was 50 µm for each slice of brain. Data collected through the microscopic system were digitally processed using an imaging MS solution software (Shimadzu). The metabolites were identified with the corresponding and fragment ion mass spectra obtained from their chemical standards. Finally, each sample was stained with HE as per a previous report.[15] Optical images of tissue sections were captured using iMScope (Shimadzu).

Statistics

Group comparisons were performed using one-way ANOVA, followed by Dunnett's multiple comparison test vs. control (GraphPad Prism 5 version 5.03; MDF, Tokyo). All data are expressed as mean ± SD, and statistical significance was set at $*P < 0.05$, $**P < 0.01$, and $***P < 0.001$.

Table 1 Mass spectrometry imaging (MSI) conditions

MSI conditions	
Analytical conditions	
Pitch	50 µm × 50 µm
Ion species	Positive ions
Measurement range	*m/z* 85–305
	m/z 520–820
Integration times	1 time/pixel
Sample voltage	3.00 kV
Detector voltage	2.10 kV
Laser irradiation conditions	
Number of irradiation	100 shots
Pulse rate	1000 Hz
Irradiation spot diameter	2
Power	45.0

iMScope was adjusted to these conditions. Each sample was analyzed two times under different measurement ranges.

Results

Histological change after tMCAO

HE staining of the section, 1.80-mm posterior to the bregma, revealed no obvious changes 1 h after tMCAO compared with controls (Figs. 1B and 1C). In contrast, neural cells in hippocampal CA1, CPu, and the cerebral cortex decreased 24 h after tMCAO. Double immunofluorescence of the TUNEL staining and NeuN with DAPI 24 h after tMCAO showed apoptosis cell death and neuronal loss in each of the three regions (Fig. 2). TUNEL-positive cells were scattered and NeuN-positive cells were decreased in CA1, CPu, and the cerebral cortex areas within the 24 h sections. The somas of NeuN-positive cells were shrunken in the CA1. In contrast, there were no such findings in these regions 1 h after tMCAO.

Profiling spectra analysis after tMCAO

The profiling spectra analysis demonstrated numerous metabolites and phospholipids, but most of them were not identified as precise substances (Fig. 3). Among them, nine ionized substances were finally identified in this analysis, namely P-Cr $[M+H]^+$ (*m/z* 212.03), Cr $[M+H]^+$ (*m/z* 132.08), Cer d18:1/18:0 $[M-H_2O+H]^+$ (*m/z* 548.54), Cer d18:1/16:0 $[M-H_2O+H]^+$ (*m/z* 520.51), Cer d18:1/20:0 $[M-H_2O+H]^+$ (*m/z* 576.57), phosphatidylcholine

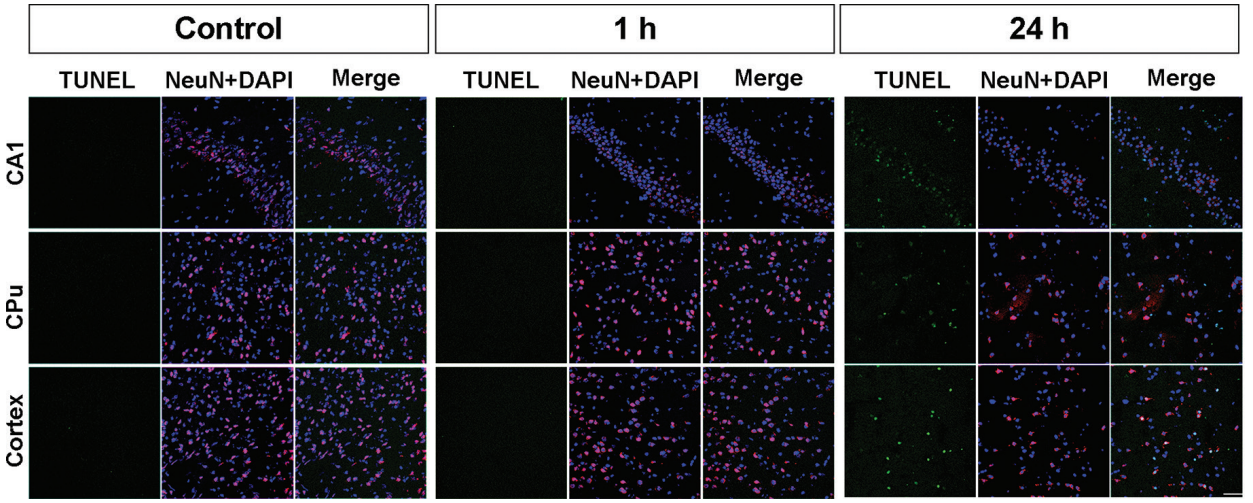

Fig. 2 Histological change after transient middle cerebral artery occlusion (tMCAO). Double immunofluorescence of the TUNEL staining (*green*) and NeuN (*red*) with DAPI (*blue*) 1 and 24 h after tMCAO. TUNEL-positive cells are scattered and NeuN-positive cells are decreased in the CA1, caudoputamen, and cerebral cortex area of a 24 h section. The soma of NeuN-positive cells appears shrunken in CA1. These findings are not seen in the 1 h section. The scale bar is 50 µm.

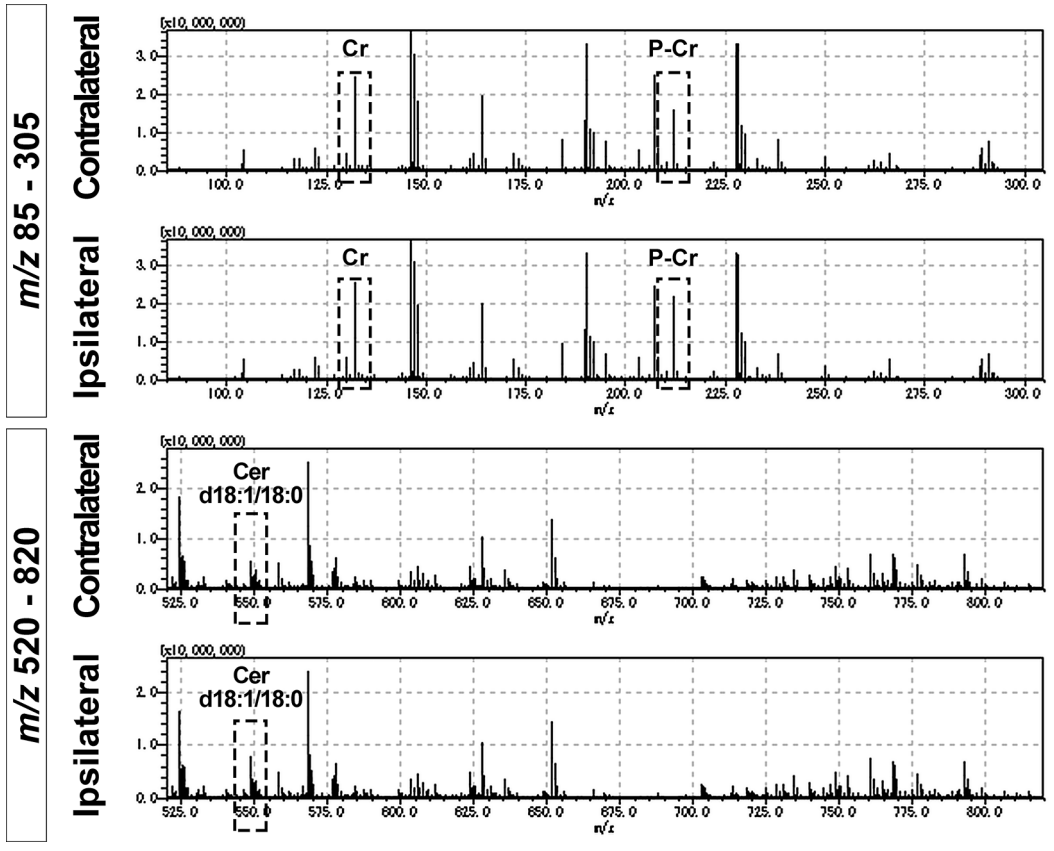

Fig. 3 Mass spectrum of mass spectrometry imaging (MSI) These graphs show four mass spectra of the ischemic and contralateral hemispheres 24 h after transient middle cerebral artery occlusion under different *m/z* scales from 85–305 and 520–820. These scan areas encompass almost entire hemispheres. MSI detects several ions within a brain section, but most of them are not identified as precise substances. *Dotted squares* indicate creatine (Cr) (*m/z* 132.08), phosphocreatine (P-Cr) (*m/z* 212.03), and ceramide (Cer) d18:1/18:0 (*m/z* 548.54). The relative intensities of P-Cr and Cer d18:1/18:0 are remarkably different between the ipsilateral and contralateral areas, but Cr exhibited no such difference.

(PC) 16:0/16:0 $[M+H]^+$ (*m/z* 734.57), PC 16:0/18:1 $[M+H]^+$ (*m/z* 760.58), L-glutamine $[M+H]^+$ (*m/z* 147.07), and L-histidine $[M+H]^+$ (*m/z* 156.08). The relative intensities of P-Cr and Cer d18:1/18:0 were remarkably different between the ipsilateral and contralateral areas, but Cr intensities exhibited no differences. Cer d18:1/18:0 was identified with the specific product ion *m/z* 264.269 on the MS/MS spectrum (data not shown), and the spectrum was the same as the previous studies.[16,17]

Tissue distribution analysis of P-Cr, Cr, and Cer d18:1/18:0 by MSI after tMCAO

Because P-Cr, Cr, and Cer d18:1/18:0 were thought to be the reproductive phospholipids in this analysis, we selected *m/z* scan ranges that corresponded to these substances for further spatial and temporal analyses after tMCAO. For acquiring spatial features, we selected sections that were 1.80-mm posterior to the bregma to simultaneously observe the hippocampus, CPu, and cerebral cortex. In the control brain, P-Cr expression levels were low throughout the entire brain. In the hippocampus, Cr expression was higher and stronger than P-Cr (Fig. 4A). One hour after tMCAO, P-Cr was upregulated in the hippocampus and CPu within the ischemic hemisphere. P-Cr also slightly increased in the ischemic cortex where it seemed to accumulate around an ischemic core. In contrast, Cr was downregulated in the hippocampus and CPu within the ischemic hemisphere (Fig. 4A). After 24 h, tMCAO, P-Cr expression was increased in the hippocampus, CPu, and ischemic cortex. Cr was slightly upregulated throughout the entire brain, with the exception of the ischemic area that showed an obvious downregulation of Cr. Cr changes did not completely correlate with P-Cr (Fig. 4A). Cer d18:1/18:0 expression was upregulated in the hippocampus 1 h after tMCAO, after which it markedly increased in the hippocampus, CPu, and cerebral cortex 24 h after tMCAO (Fig. 4A). Focusing on the ischemic cores of the hippocampus, CPu, and cortex, P-Cr and Cer d18:1/18:0 expression increased over time, whereas Cr expression exhibited no such tendency (Fig. 4B). Only Cer d18:1/18:0 expression of CPu was significantly different between the control and 24 h after reperfusion samples in the present analysis. The relative intensities were measured within the three regions of interest presented in the optical image and contralateral sides. These graphs indicate the contralateral ratio of the relative intensities.

Discussion

In this study, we detected several ionized substances in the ranges of *m/z* targeting P-Cr, Cr, and Cer d18:1/18:0 in the hippocampal CA1, CPu, and cerebral cortex early after tMCAO in a single analysis. P-Cr and Cer d18:1/18:0 expressions were upregulated 1 h after tMCAO, whereas no changes were evident on HE staining and immunofluorescence assay. Further, P-Cr and Cer d18:1/18:0 increased with time, followed by neuronal loss.

Individual differences in the collateral circulation alter metabolism and the areas of infarction after MCAO.[18,19] Additionally, metabolic biomolecule distributions are significantly altered relative to the survival time following disease onset.[20] Therefore, to understand the precise disease states, it is necessary to acquire additional information pertaining to biomolecules within the area of interest.[20] In this study, we assessed ischemic conditions using HE staining and immunofluorescence. HE staining showed that neural cells within the hippocampal CA1, CPu, and cerebral cortex decreased 24 h after tMCAO. Immunofluorescence 24 h after tMCAO showed cell death in all the three regions. These findings indicate the CA1, CPu, and cerebral cortex were injured in our tMCAO model.

P-Cr and Cr are thought to contribute to cell life and death. P-Cr is formed from Cr and catalyzed by Cr kinase.[21] Under anoxic or ischemic conditions, adenosine triphosphate (ATP) supplies are decreased; however, P-Cr functions as an energy source for cellular activity by releasing its phosphate group to adenosine diphosphate (ADP).[22,23] Several studies have reported that P-Cr can cross the blood–brain barrier and the cell membrane, exerting neuroprotective effects.[24–27] In our study, MSI revealed temporal increases of P-Cr and Cer d18:1/18:0 after tMCAO in ischemic cores. In contrast, Cr changes did not completely correlate with P-Cr changes. Although the dynamics and metabolic activity of Cr are complex and remain poorly elucidated, P-Cr may be a target for molecular therapy as well as a biomarker for acute cerebral ischemia.

Cer d18:1/18:0 also contributes to cell life and death. The synthase of Cer d18:1/18:0 is essential to cell life, and the hydrolysis of sphingomyelin is instrumental in apoptosis.[28] A few studies have reported Cer d18:1/18:0 accumulation during acute and chronic ischemia as a result of brain injury.[29–31] In our study, Cer d18:1/18:0, as well as P-Cr, were detected by MSI 1 h after tMCAO, although no changes were evident on HE staining and immunofluorescence. Therefore, the upregulation of P-Cr and Cer d18:1/18:0 can be an early biomarker for cerebral ischemia and can be utilized in neuroprotective therapies. Apparently, it is difficult to perform MALDI-MSI analysis of a living human body, but the results can be applied through magnetic resonance spectroscopy.[32]

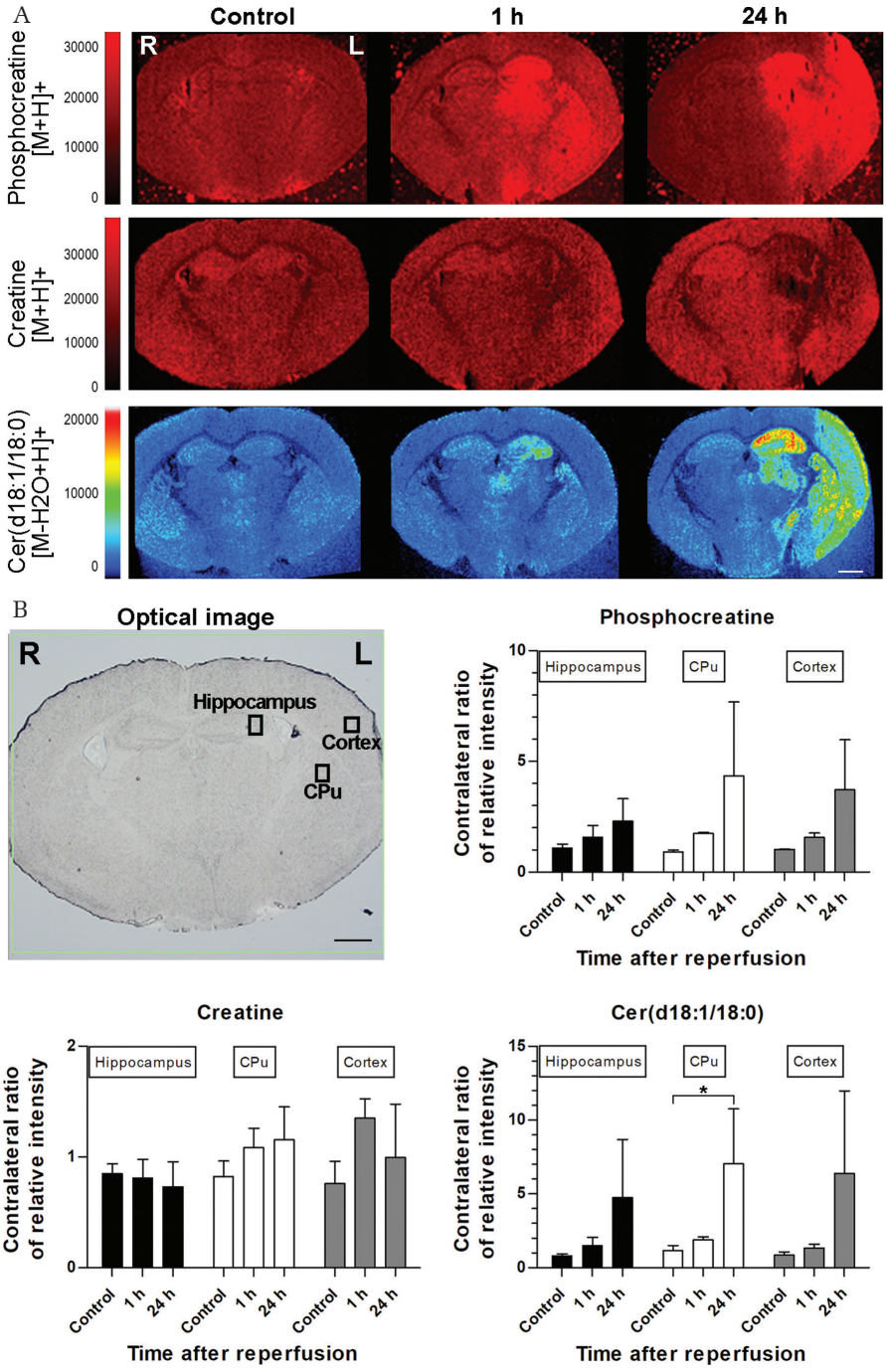

Fig. 4 Mass spectrometry imaging (MSI) at different time points (A). Time course MSI analysis of phosphocreatine (P-Cr), creatine (Cr), and ceramide (Cer) d18:1/18:0 after transient middle cerebral artery occlusion (tMCAO) at 1.80 mm posterior to the bregma. In the control brain, P-Cr expression is low throughout the entire brain. Cr expression is higher than P-Cr and is stronger in the hippocampus. One hour after tMCAO, P-Cr expression is upregulated in the hippocampus, caudoputamen (CPu), and cerebral cortex of the ischemic hemisphere. In contrast, Cr expression is downregulated in the hippocampus and CPu of the ischemic hemisphere. Cer d18:1/18:0 expression is upregulated in the hippocampus. After 24 h, tMCAO, P-Cr, and Cer d18:1/18:0 expressions are increase in the hippocampus, CPu, and ischemic cortex. Cr expression is slightly upregulated throughout the entire brain, with the exception of the ischemic area, which shows an obvious downregulation of Cr. (B) The relative intensities were measured at three regions of interests presented in the optical image and contralateral sides. These graphs indicate the contralateral ratio of relative intensity. P-Cr and Cer d18:1/18:0 expressions increase over time, but Cr expression exhibits no such tendency. *$P < 0.05$. Each group included three samples. The scale bars are 1000 μm.

Conclusion

We describe the spatial and temporal metabolite expression following tMCAO by MALDI-MSI without any staining. P-Cr and Cer d18:1/18:0 accumulated over time in the ischemic core and surrounding areas after ischemia. The upregulation of P-Cr and Cer d18:1/18:0 was detected 1 h after tMCAO when no changes were evident on HE staining and immunofluorescence assay. Thus, P-Cr and Cer d18:1/18:0 can be utilized in neuroprotective therapies as biomarker candidates for cerebral ischemia.

Acknowledgments

Natsumi Konno provided invaluable technical support for this project. This study was partially supported by JSPS KAKENHI Grant Number 17H01583 from the Japan Agency for Medical Research and

Development, AMED. The authors would like to thank Enago (www.enago.jp) for the English language review.

Conflicts of Interest Disclosure

The authors have no conflicts of interest to disclose.

References

1) Irie M, Fujimura Y, Yamato M, Miura D, Wariishi H: Integrated MALDI-MS imaging and LC-MS techniques for visualizing spatiotemporal metabolomic dynamics in a rat stroke model. *Metabolomics* 10: 473–483, 2014
2) Mulder IA, Esteve C, Wermer MJ, et al.: Funnel-freezing versus heat-stabilization for the visualization of metabolites by mass spectrometry imaging in a mouse stroke model. *Proteomics* 16: 1652–1659, 2016
3) Pohjanen E, Thysell E, Jonsson P, et al.: A multivariate screening strategy for investigating metabolic effects of strenuous physical exercise in human serum. *J Proteome Res* 6: 2113–2120, 2007
4) Werner E, Croixmarie V, Umbdenstock T, et al.: Mass spectrometry-based metabolomics: accelerating the characterization of discriminating signals by combining statistical correlations and ultrahigh resolution. *Anal Chem* 80: 4918–4932, 2008
5) Stoeckli M, Chaurand P, Hallahan DE, Caprioli RM: Imaging mass spectrometry: a new technology for the analysis of protein expression in mammalian tissues. *Nat Med* 7: 493–496, 2001
6) Amstalden van Hove ER, Smith DF, Heeren RM: A concise review of mass spectrometry imaging. *J Chromatogr A* 1217: 3946–3954, 2010
7) Miura D, Fujimura Y, Yamato M, et al.: Ultrahighly sensitive in situ metabolomic imaging for visualizing spatiotemporal metabolic behaviors. *Anal Chem* 82: 9789–9796, 2010
8) Vickerman JC: Molecular imaging and depth profiling by mass spectrometry—SIMS, MALDI or DESI? *Analyst* 136: 2199–2217, 2011
9) Roux A, Muller L, Jackson SN, et al.: Mass spectrometry imaging of rat brain lipid profile changes over time following traumatic brain injury. *J Neurosci Methods* 272: 19–32, 2016
10) Whitehead SN, Chan KH, Gangaraju S, Slinn J, Li J, Hou ST: Imaging mass spectrometry detection of gangliosides species in the mouse brain following transient focal cerebral ischemia and long-term recovery. *PLoS ONE* 6: e20808, 2011
11) Ito A, Niizuma K, Shimizu H, Fujimura M, Hasumi K, Tominaga T: SMTP-7, a new thrombolytic agent, decreases hemorrhagic transformation after transient middle cerebral artery occlusion under warfarin anticoagulation in mice. *Brain Res* 1578: 38–48, 2014
12) Chen Y, Ito A, Takai K, Saito N: Blocking pterygopalatine arterial blood flow decreases infarct volume variability in a mouse model of intraluminal suture middle cerebral artery occlusion. *J Neurosci Methods* 174: 18–24, 2008
13) Murakami K, Kondo T, Kawase M, Chan PH: The development of a new mouse model of global ischemia: focus on the relationships between ischemia duration, anesthesia, cerebral vasculature, and neuronal injury following global ischemia in mice. *Brain Res* 780: 304–310, 1998
14) Pulsinelli WA, Brierley JB, Plum F: Temporal profile of neuronal damage in a model of transient forebrain ischemia. *Ann Neuro* 11: 491–498, 1982
15) Hattori K, Kajimura M, Hishiki T, et al.: Paradoxical ATP elevation in ischemic penumbra revealed by quantitative imaging mass spectrometry. *Antioxid Redox Signal* 13: 1157–1167, 2010
16) Hankin JA, Farias SE, Barkley RM, et al.: MALDI mass spectrometric imaging of lipids in rat brain injury models. *J Am Soc Mass Spectrom* 22: 1014–1021, 2011
17) Murphy RC, Axelsen PH: Mass spectrometric analysis of long-chain lipids. *Mass Spectrom Rev* 30: 579–599, 2011
18) Kitagawa K, Matsumoto M, Yang G, et al.: Cerebral ischemia after bilateral carotid artery occlusion and intraluminal suture occlusion in mice: evaluation of the patency of the posterior communicating artery. *J Cereb Blood Flow Metab* 18: 570–579, 1998
19) Wellons JC, Sheng H, Laskowitz DT, Mackensen GB, Pearlstein RD, Warner DS: A comparison of strain-related susceptibility in two murine recovery models of global cerebral ischemia. *Brain Res* 868: 14–21, 2000
20) Matsumoto K, Graf R, Rosner G, Taguchi J, Heiss WD: Elevation of neuroactive substances in the cortex of cats during prolonged focal ischemia. *J Cereb Blood Flow Metab* 13: 586–594, 1993
21) Wyss M, Kaddurah-Daouk R: Creatine and creatinine metabolism. *Physiol Rev* 80: 1107–1213, 2000
22) Perasso L, Cupello A, Lunardi GL, Principato C, Gandolfo C, Balestrino M: Kinetics of creatine in blood and brain after intraperitoneal injection in the rat. *Brain Res* 974: 37–42, 2003
23) Rawson ES, Venezia AC: Use of creatine in the elderly and evidence for effects on cognitive function in young and old. *Amino Acids* 40: 1349–1362, 2011
24) Balestrino M, Sarocchi M, Adriano E, Spallarossa P: Potential of creatine or phosphocreatine supplementation in cerebrovascular disease and in ischemic heart disease. *Amino Acids* 48: 1955–1967, 2016
25) Prabhakar G, Vona-Davis L, Murray D, Lakhani P, Murray G: Phosphocreatine restores high-energy phosphates in ischemic myocardium: implication for off-pump cardiac revascularization. *J Am Coll Surg* 197: 786–791, 2003
26) Pattillo RA, Collier BD, Abdel-Dayem H, et al.: Phosphorus-32-chromic phosphate for ovarian cancer: I. Fractionated low-dose intraperitoneal treatments in conjunction with platinum analog chemotherapy. *J Nucl Med* 36: 29–36, 1995

27) Li T, Wang N, Zhao M: Neuroprotective effect of phosphocreatine on focal cerebral ischemia-reperfusion injury. *J Biomed Biotechnol* 2012: 168756, 2012
28) Birbes H, El Bawab S, Hannun YA, Obeid LM: Selective hydrolysis of a mitochondrial pool of sphingomyelin induces apoptosis. *FASEB J* 15: 2669–2679, 2001
29) Nakane M, Kubota M, Nakagomi T, et al.: Lethal forebrain ischemia stimulates sphingomyelin hydrolysis and ceramide generation in the gerbil hippocampus. *Neurosci Lett* 296: 89–92, 2000
30) Novgorodov SA, Gudz TI: Ceramide and mitochondria in ischemic brain injury. *Int J Biochem Mol Biol* 2: 347–361, 2011
31) Ohtani R, Tomimoto H, Kondo T, et al.: Upregulation of ceramide and its regulating mechanism in a rat model of chronic cerebral ischemia. *Brain Res* 1023: 31–40, 2004
32) Lin AQ, Shou JX, Li XY, Ma L, Zhu XH: Metabolic changes in acute cerebral infarction: Findings from proton magnetic resonance spectroscopic imaging. *Exp Ther Med* 7: 451–455, 2014

Address reprint requests to: Kuniyasu Niizuma, MD, PhD, Department of Neurosurgical Engineering and Translational Neuroscience, Graduate School of Biomedical Engineering, Tohoku University, 1-1 Seiryo-machi, Aoba-ku, Sendai, Miyagi 980-8574, Japan.
e-mail: niizuma@nsg.med.tohoku.ac.jp